Wiley Online Library
Early View publication on www.wileyonlinelibrary.com
(issue and page numbers not yet assigned;
citable using Digital Object Identifier – **DOI**)

Phys. Status Solidi B, 1–8 (2015) / **DOI** 10.1002/pssb.201552414

physica status solidi b
www.pss-b.com
basic solid state physics

Self-consistent hybridization expansions for static properties of the Anderson impurity model

I. J. Hamad[1], **P. Roura-Bas**[*,2], **A. A. Aligia**[3], and **E. V. Anda**[4]Q1

[1] Consejo Nacional de Investigaciones Científicas y Técnicas, CONICET, and Universidad Nacional de Rosario, Argentina
[2] Depto de Física CAC-CNEA and Consejo Nacional de Investigaciones Científicas y Técnicas, CONICET, Argentina
[3] Comisión Nacional de Energía Atómica, Centro Atómico Bariloche and Instituto Balseiro, 8400 S.C Bariloche, Argentina
[4] Pontificia Universidade Catolica, Rio de Janeiro, Brazil

Received 22 June 2015, revised 14 September 2015, accepted 16 September 2015
Published online 00 Month 2015

Keywords Anderson impurity model, ground-state properties, Kondo effect

[*] Corresponding author: e-mail roura@tandar.cnea.gov.ar, Phone: +54-11 67727096Q2

Building an effective Hamiltonian utilizing a projector-operator procedure, we derive an approximation based on a self-consistent hybridization expansion to study the ground state properties of the Anderson Impurity model. We applied the approximation to the general case of finite Coulomb repulsion U, extending previous work with the same formalism in the infinite-U case. The ground state energy and their related zero temperature properties are accurately obtained in the case in which U is large enough, but still finite, as compared with the rest of energy scales involved in the model. The results for the valence of the impurity are compared with exact results that we obtain from equations derived using the Bethe ansatz and with a perturbative approach. The magnetization and magnetic susceptibility is also compared with Bethe ansatz results. In order to do this comparison, we also show how to regularize the Bethe ansatz integral equations necessary to calculate the impurity valence, for arbitrary values of the parameters.

1 Introduction The Anderson impurity model (AIM) [1], which is one of the most studied Hamiltonians including strong correlations in condensed-matter physics, has been solved exactly by means of the Bethe ansatz [2, 3]. In addition, the spectral function and many other correlation functions have been accurately computed by using the numerical renormalization group (NRG) [4, 5].

However, several approximated schemes are also used. Frequently, they shed light on the expected behavior of some properties and can be used to fit experiments, when due to a large number of degrees of freedom it is not possible to use more robust but also time-consuming techniques. Moreover, there is no Bethe ansatz solution in the case of a frequency-dependent hybridization function. Among the approximations, the self-consistent hybridization (SCH) expansions for solving the AIM are commonly used within a large class of different problems. The noncrossing approximation, NCA [6] which represents the simplest family of these self-consistent treatments, provides an accurate calculation of the Green functions, as well as many other properties, when the Coulomb repulsion is taken to be infinite. Since the 80's the NCA has been successfully applied to study Ce compounds [7], nonequilibrium transport properties [8] and, more recently, non-Fermi liquid behaviors [9], electron–phonon interaction [10], and spectroscopy of a double quantum dot system [11].

When the Coulomb repulsion U takes a finite value, the NCA has failed to give the correct Kondo scale (T_K). Unfortunately, its value is found to be very underestimated as compared with the correct one obtained from the Bethe ansatz solution of the model. The next leading order in the self-consistent expansions that partially solves this pathology is often known as the one crossing approximation, OCA [12–14]. Within this extended formalism, other classes of problems have been successfully investigated [15]. Among them, its mayor application is in the context of the dynamical mean-field theory as an impurity solver [16].

However, the use of NCA or OCA approximations imposes some limitations. Finite temperatures T have to be used, specifically temperatures larger than $0.01T_K$ in the

former and $0.1T_K$ in the later, in order to avoid an artificial increase by about 10% in the spectral weight at the Fermi level. The same pathology arises when these techniques are applied to systems in which the ground state without hybridization is a nondegenerate state. This is the case when either the impurity state is empty (or formed by an even number of electrons) or when a magnetic field is applied to the impurity that brakes the Kramers degeneracy (Zeeman effect).

Remarkably, these limitations when calculating dynamical properties are absent in the case of static ones [17] like those derived from the ground state energy. In the early approach given by Inagaki [18] and Keiter and Kimball [19], the valence of the impurity as well as the charge and spin susceptibilities were calculated from the ground state energy ($T = 0$) in the U infinite limit and for a large value of the conduction bandwidth $D \to \infty$.

Recently, an improvement of these calculations incorporating higher order processes when calculating the occupancy and magnetization of the impurity was done by three of us [20]. The agreement with exact results was remarkable.

However, an extension of this static approximation to finite values of U is still desirable. This is justified due to the existence of relatively not so large values of the Coulomb interaction in bulk systems as well as in systems of semiconductor quantum dots or carbon nanotubes through which transport experiments are currently being performed [21, 32, 33].

In this contribution, we extend the use of the SCH expansions when calculating the ground state properties of the single impurity Anderson model to incorporate large but finite values of the Coulomb repulsion. We compare our approximated ground state properties, like valence and magnetization of the impurity with exact Bethe ansatz calculations. We also provide a method to regularize the divergences that appear in some Bethe ansatz expressions which might be useful for researchers interested in using these exact results. In addition, in the opposite limit, we start the discussion showing the excellent agreement of impurity occupancy calculated from perturbation theory (PT) to second order in U, modified to give the correct result in the atomic limit and to satisfy the Friedel sum rule [22, 23], for not so large values of U as compared with the hybridization strength.

The outline is as follows: In Section 2, the model is introduced and, starting from a projector-operator procedure, the self-consistent hybridization expansion including finite values of the Coulomb repulsion is reviewed. We generalize the self-consistent hybridization expansion to include finite values of the Coulomb repulsion. Section 3 presents the numerical results for different physical magnitudes, including a detailed benchmark between Bethe ansatz results and the approximated PT and SCH-expansion. Finally, in Section 4 some conclusions are drawn. In the appendix, we explicitly give the steps that we follow in order to regularize and compute in an efficiently numerical way the integral equations of the Bethe ansatz when calculating the impurity valence for arbitrary values of the model parameters.

2 Model and formalism

We work with the Anderson Hamiltonian,

$$H = \sum_{k\sigma} \epsilon_k n_{k\sigma} + \sum_{\sigma} E_d n_{d\sigma} + U n_{d\uparrow} n_{d\downarrow} + \sum_{k\sigma} (V_k d_\sigma^\dagger c_{k\sigma} + \text{H.c.}), \quad (1)$$

where $n_{k\sigma} = c_{k\sigma}^\dagger c_{k\sigma}$ is the number operator for conduction electrons, $c_{k\sigma}^\dagger$ creates a conduction electron with momentum k and spin σ, and $n_{d\sigma} = d_\sigma^\dagger d_\sigma$ and $d_\sigma^\dagger$ are the analogous operators for electrons in the localized impurity, which has a local energy E_d and Coulomb repulsion U. The coupling of the impurity with the conduction band is given by the hybridization function $\Delta(\omega) \equiv \pi \sum_k V_k^2 \delta(\omega - \epsilon_k)$. We focus on the energy of the ground state, E_0, of the system with a ground state wavefunction $|\psi_0\rangle$. From it, other quantities such as the occupancy of the impurity, magnetization, and susceptibility can be obtained, after incorporating a magnetic field B via a Zeeman term $g\mu_B B(n_\downarrow - n_\uparrow)/2$ in the Hamiltonian.

The procedure we follow in general is the same as the one applied in a previous work by three of us [20]. The main idea is to divide the Hilbert space in two subspaces, by means of projector operators, but with the peculiarity that the working subspace consists of a single state. For that purpose, we define the projector operator $P_1 = \prod_{k\sigma \le k_F} n_{k\sigma}$, being k_F the Fermi wave vector, and $P_2 = 1 - P_1$. These projectors then divide the Hilbert space of the system into two disjoint subspaces: S_1, which contains only one state corresponding to the Fermi sea with no electrons in the d-level, $|\phi_1\rangle = \prod_{k\sigma \le k_F} c_{k\sigma}^\dagger |0\rangle$, and S_2, that contains the rest of the states in the Hilbert space. In principle, the state $|\phi_1\rangle$ can be chosen as either the one in which the impurity is empty, singly, or doubled occupied, arriving at the same final results.

The effective Hamiltonian that operates on the S_1 subspace obeys the equation [20]

$$\tilde{H}|\phi_1\rangle = \left(H_{11} + H_{12} \frac{1}{E - H_{22}} H_{21} \right) |\phi_1\rangle = E|\phi_1\rangle, \quad (2)$$

where $H_{ij} = P_i H P_j$. The term H_{21} comes from the hybridization term and so connects the subspace S_1 with S_2. It acts creating a singlet state belonging to the S_2 subspace,

$$|\phi_{kd}\rangle = \sum_\sigma \frac{d_\sigma^\dagger c_{k\sigma}}{\sqrt{2}} |\phi_1\rangle, \quad (3)$$

We label k and K the wave numbers below and above the Fermi level, respectively. We obtain the equation for the energy after applying $\langle\phi_1|$ to the left of Eq. (2)

$$E = \epsilon_T + 2\frac{V^2}{N} \sum_{k,k'} \left\langle \phi_{kd} \left| \frac{1}{E - H_{22}} \right| \phi_{k'd} \right\rangle, \quad (4)$$

where $\epsilon_T = 2\sum_k \epsilon_k$ represents the energy of the ground state of the Fermi sea. As usual, we neglect the k dependence of $V_k = V/\sqrt{N}$.

As we stated in the previous work [20], in order to get an explicit expression for the eigenvalues in (4), it is enough to calculate the matrix elements of the operator $(E - H_{22})^{-1}$ between the states $|\phi_{kd}\rangle$. These states are created by a single application of the H_{12} term of the Hamiltonian to $|\phi_1\rangle$ in the S_1 subspace. Besides, as the space S_2 is created by successive applications of the Hamiltonian, and this commutes with the total spin operator, the subspace S_2 contains only states that are singlets.

Up to this point, the procedure has been completely general and equal to the one presented in previous work done in the infinite U case [20]. Now, in order to generalize the treatment we consider arbitrary values of U, and hence processes where the impurity is doubly occupied.

Although it is in principle possible to obtain all the matrix elements g_{ij} of the resolvent operator $G = (E - H_{22})^{-1}$, it can be noticed that to calculate the ground state energy, given in (4), it is only necessary to calculate the diagonal g_{kk} and nondiagonal matrix elements $g_{kk'}$ corresponding to the states below the Fermi level. Following closely the treatment done in [20], and working in the thermodynamic limit, we begin by examining only the diagonal contribution g_{kk}, which is expressed as a continuous fraction that ultimately, in the thermodynamic limit, can be written in a closed expression as follows:

$$g_{kk}(E) = \frac{1}{E + \epsilon_k - E_d - F_0(E+\epsilon_k) - F_2(E+\epsilon_k)}, \quad (5)$$

where the functions F_0 and F_2 satisfy a set of three self-consistent equations, exact up to terms proportional to V^2.

$$\begin{aligned} F_0(E) &= \frac{V^2}{N}\sum_K \frac{1}{E - \epsilon_K - F_1(E-\epsilon_K)} \\ F_1(E) &= 2\frac{V^2}{N}\sum_k \frac{1}{E + \epsilon_k - E_d - F_0(E+\epsilon_k) - F_2(E+\epsilon_k)}. \\ F_2(E) &= \frac{V^2}{N}\sum_k \frac{1}{E + \epsilon_k - 2E_d - U - F_1(E+\epsilon_k)}. \end{aligned} \quad (6)$$

The system of equations incorporates an extra function, F_2, not present in the infinite U case, related to processes in which the impurity is doubly occupied.

The ground state energy, according to Eqs. (4), (5), and (6), can be self consistently expressed by,

$$E = F_1(E) \quad (7)$$

The solution of these equations incorporates processes of all orders in the hopping matrix element V. However, the ground state energy obtained still remains perturbative, even though the second-order processes are re-summed self-consistently. Going beyond the self-consistent second-order approximation, given by the diagonal term g_{kk}, we incorporate the next leading order taking into account the nondiagonal elements $g_{kk'}$, to the calculation of the ground state energy. Instead of incorporating this crossing terms self consistently into Eq. (6), which is a difficult numerical task, we express this nondiagonal contribution to the energy in terms of the auxiliary functions F_0, F_1, and F_2 calculated as we proposed above.

$$Q_1(E) = 2\frac{V^2}{N}\sum_{k,k'\neq k} g_{kk'}(E), \quad (8)$$

with $g_{kk'}$ given by

$$\begin{aligned} g_{kk'}(E) = \frac{V^2}{N} &\frac{1}{E + e_k - E_d - F_0(E+e_k) - F_2(E+e_k)} \\ &\times \frac{1}{E + e_k + e_{k'} - 2E_d - U - F_1(E + e_k - e_{k'})} \\ &\times \frac{1}{E + e_{k'} - E_d - F_0(E+e_{k'}) - F_2(E+e_{k'})}. \end{aligned} \quad (9)$$

Including this nondiagonal term, we obtain the next leading order contribution to the energy, which is proportional to V^4.

$$E = F_1(E) + Q_1(E) \quad (10)$$

In general, when solving Eq. (10) there are three solutions but only one lies below E_d, which corresponds to the ground state energy. Regarding the numerical algorithm employed in searching for the solution, it is similar to the one used in the standard NCA approximation, that is the use of logarithmic meshes with a strong dense region around the energy position of the ground state, and this position is dynamically changed iteration after iteration until convergence.

The method can be straightforwardly generalized to an Anderson model with an $SU(N)$ symmetry without any additional numerical cost. In fact, the self-consistent system of equations in Eq. (6) can be easily modified to be the solution of the $2-$level infinite$-U$ Anderson model, which in the case of degenerate and equally hybridized levels represents the $SU(4)$ Anderson model, which is nowadays the focus of intense experimental and theoretical research [32]. Note that when solving $SU(N)$ models with NRG, the Hilbert space increases by 2^N at each iteration, rendering the calculation very difficult for $N = 4$ and almost impossible for $N > 4$. There is also no important computational cost in breaking $SU(N)$ symmetry within our method.

In what follows, we discuss the impurity properties derived by the numerical solution of the Eq. (10).

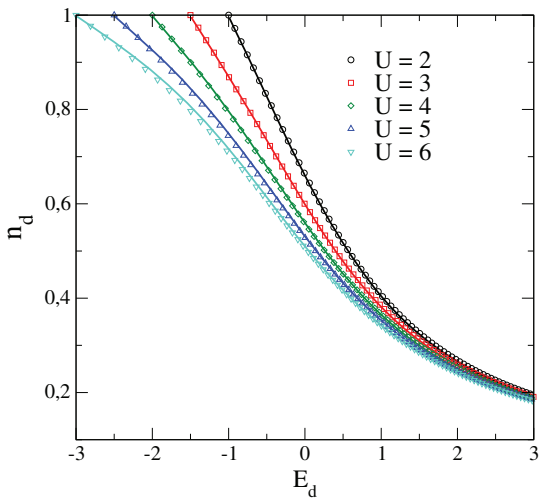

Figure 1 Impurity occupation as a function of E_d. Solid lines stand for the Bethe ansatz results while symbols indicate the results from PT.

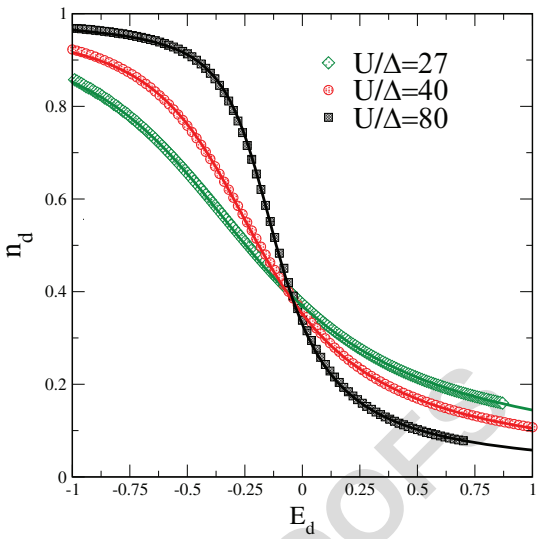

Figure 2 Total impurity occupancy as a function of the energy level E_d in the strong interacting limit for several values of the Coulomb repulsion U. Solid lines stand for the Bethe ansatz results.

3 Numerical results We employ a square hybridization of intensity Δ with a half-bandwidth D, which is related with the hopping V via $\Delta = \pi V^2/2D$. Furthermore, we chose $\Delta = 1$ as our unit of energy.

3.1 Ground state energy and impurity valence

As we state in the introduction, it is important for many applications to get a simple approximation that can be used, when the Coulomb repulsion is large enough but still finite, for an examination of the magnitudes derived from the ground state energy, such as the valence of the impurity.

On the other hand, when the Coulomb repulsion is not too large, that is, of the order of the hybridization energy Δ, perturbation theory in the parameter U provides accurate results. For instance, renormalized-PT has been successfully used to analyze the temperature and voltage universal dependence of the conductance [24, 25]. Specifically, in Fig. 1 we show the total occupancy of the impurity obtained from PT improved in such a way that it reproduces the atomic limit and satisfies the Friedel sum rule for all occupancies [22, 23], and the exact one calculated from the Bethe ansatz (see Appendix) for several values of U as a function of the impurity energy E_d.

As it can be seen from Fig. 1, the impurity occupation obtained from PT only presents small deviations as compared with the exact ones (less than 1%) when the Coulomb repulsion is set to be $U = 6\Delta$. Unfortunately, the deviations from the exact values quickly grow in the strong interacting limit, when the Coulomb repulsion is several orders of magnitude larger than Δ. Also our results (not shown) indicate that the magnetic susceptibility within the modified PT approach underestimates the magnetic susceptibility by more than 6% for $U \geq 3\Delta$ in the symmetric case $E_d = -U/2$.

This situation emphasizes the convenience of having an approach capable of studying the strong interacting limit, $U >> \Delta$, since it represents a realistic case of most semiconductor and molecular quantum dots. The SCH expansion we propose to calculate the ground state energy, impurity occupation, magnetization, and susceptibility satisfies this condition. In what follows, we present our main results.

Figure 2 shows the impurity occupation as a function of the local level E_d for several values of U calculated from the SCH expansion including the 4th order processes. The solid lines indicate the results obtained from the Bethe ansatz technique. We include an appendix in which we explicitly show the steps we follow to compute the integral expressions that determine the valence within the Bethe ansatz solution for arbitrary values of the model parameters. Here, we have changed the unit of energy $\Delta = 1$ by setting $\Delta = 0.1; 0.2$ and 0.3 while we chose $U = 8$.

In Fig. 3, we plot the SCH results for the impurity occupancy shown in Fig. 2 as a function of the renormalized energy $E_d^* = E_d + \frac{\Delta}{\pi}\ln(\frac{\pi eU}{4\Delta})$ which explicitly includes the Haldane shift [27] together with the corresponding renormalized Bethe ansatz curve. As expected from the universality of the model, we notice here that all the curves collapse into an universal one in the Kondo regime $-E_d^* \gg \Delta$ and that at $E_d^* = 0$ the valence is $n_d = 0.58$ in agreement with Fig. 2 of Ref. [2].

3.2 Magnetic properties

In what follows, by adding a magnetic field B to the Hamiltonian 1, we study the impurity contribution to the magnetization, $M_{\rm imp}$. The inclusion of the Zeeman interaction within the SCH procedure is straightforward and it is described in Ref. [20]. The impurity magnetization can be obtained by deriving of the ground state energy with respect to the magnetic field and removing from

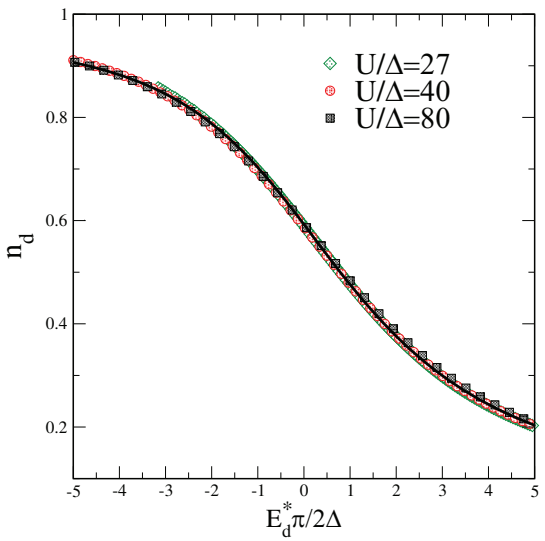

Figure 3 Universal occupation number n_d as a function of the scaled energy $\pi E_d^*/2\Delta$ for the same parameters that in Fig. 2.

this the conduction band contribution,

$$M_{\rm imp}(B) = -\frac{\partial}{\partial B}(E(B) - \epsilon_T(B)). \tag{11}$$

Figure 4 shows the SCH results of $M_{\rm imp}$ in units of $g\mu_B$ as a function of B/T_1 for $U = 12$ in the symmetric case $E_d = -6$, compared with the exact Bethe ansatz results for the Kondo model [29]. This is justified since for the symmetric case charge fluctuations are frozen and the Anderson model maps onto the Kondo one.

The Kondo regime is characterized by the energy scale T_1 [29], and its relation with the susceptibility at zero temperature is given by

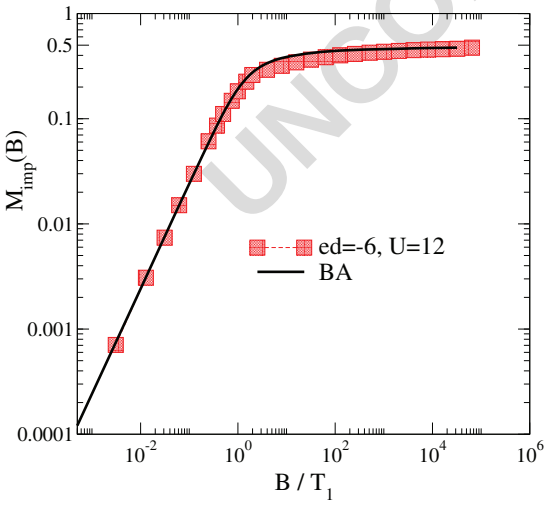

Figure 4 Comparison of the results obtained by the SCH expansion for $M_{\rm imp}$, in units of $g\mu_B$ and as a function of B/T_1, for the symmetric case with those from the Bethe ansatz solution of the Kondo model. The scale T_1 is defined in the main text.

$$\chi_{\rm imp}(B=0) \equiv \frac{\sqrt{2\pi e}}{T_1}. \tag{12}$$

It can be noticed from Fig. 4 that the agreement between SCH expansion and BA is very good when $M_{\rm imp}$ is calculated in units of B/T_1, for which $M_{\rm imp}$ is a universal curve. In particular, the SCH approach captures both the linear dependence of the magnetization for small values of B, which is a signature of the Kondo effect, and the logarithmic dependence for larger ones [29, 3, 30].

The Kondo scale, $T_{\rm K}$, is also frequently found from the susceptibility at zero magnetic field $\chi_{\rm imp}(B=0) \propto \frac{1}{T_{\rm K}}$, and Eq. (12) permits a relation between both energy scales, $T_1 = 4\sqrt{2\pi e}\, T_{\rm K}$. Unfortunately, outside the regime $U \gg |E_d|, \Delta$, the Kondo scale that we obtain within the SCH procedure is found to be several orders of magnitude smaller than the one corresponding to the Haldane scale, $T_{\rm K} = \sqrt{\frac{U\Delta}{2}} exp(-\frac{\pi U}{8\Delta})$ [27], for the symmetric case. For the parameters used in Fig. 4, the SCH expansion predicts a Kondo scale of the order of 10^{-5} while the corresponding one to the Haldane expression is of the order of 10^{-2} in units of Δ.

Therefore, outside the regime $U \gg |E_d|, \Delta$, the SCH expansion to obtain the ground state energy, within the approximation proposed, requires the calculation of the Kondo temperature using other approaches.

This is not a surprising result. The same feature appears when the SCH expansion in its lowest version, NCA, is applied using finite values of the Coulomb interaction [12–14]. As we mentioned in the introduction, this pathology was partially overcome adding, in a self-consistent way, all the dressed diagrams that involve one crossing conduction electrons, which corresponds to the next leading order called one-crossing approximation OCA. While in our present treatment of the problem, we are already taking into account 4th order processes, we are not including these contributions in a self-consistent way, as we mentioned in Section 2 and can be seen from Eq. (6). While our treatment is completely reliable to obtain the static properties of the Anderson Hamiltonian for $U \gg \Delta, |E_d|$, it fails to give correctly the Kondo temperature when U/Δ is not large enough, situation in which an equivalent scheme to OCA approximation is required. This full treatment is beyond the scope of the present study.

As a final analysis, we include in Fig. 5 the susceptibility comparing our results for $\chi_{\rm imp}$ with those obtained from a Bethe ansatz calculation [31] in the case of infinite Coulomb repulsion U. Note that the Haldane shift [28] (introduced before when discussing Fig. 3) diverges when both D and U are infinite. Therefore, in the Bethe ansatz calculation, only the renormalized energy level E_d^* which contains this shift, keeps a physical meaning. In the left panel of Fig. 5, we show results of the SCH method for both $D = 10$ and $D \to \infty$ shifted by a constant energy $E_d^* - E_d$ so that the results coincide with the Bethe ansatz solution for $\chi_{\rm imp}$. The agreement with the latter is very good in both cases, capturing

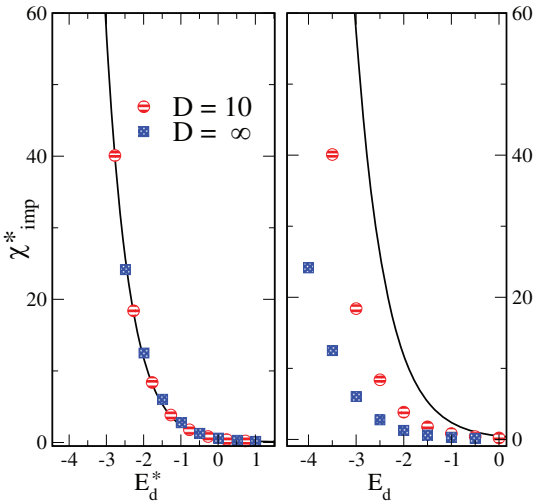

Figure 5 Left: Impurity contribution to magnetic susceptibility $\chi^* = \chi/((\mu_B g)^2/\Delta)$ as a function of the renormalized energy E_d^*. The solid line indicates the calculation by using the Bethe ansatz technique in the limit of both, $D, U \to \infty$. The symbols represent the SCH solution for two values of the bandwidth D. Right: same as before in terms of the unrenormalized energy E_d for the SCH results.

the universality of the model. For completeness, the right panel of the figure shows the values of the susceptibility as calculated from the SCH method, without shifting the energy.

4 Summary and conclusions In this work, we applied the self-consistent hybridization expansions including 4th order processes to compute the ground state energy, occupancy, and magnetic properties of the Anderson impurity model in the case of finite Coulomb repulsion, extending a previous treatment for infinite U. We show that the static properties of the model can be well calculated within the SCH expansions for zero temperature and finite magnetic fields. We successfully match our results with those coming from the Bethe ansatz solution of the model.

This simple approach allows the study of systems that can be described by the Anderson model, such as semiconductor [32] or molecular quantum dots [33] where the Coulomb repulsion is expected to be large but cannot be considered infinite. Experimentally relevant quantities, such as the equilibrium conductance of the impurity, which is directly related to the occupancy (if the system is in a Fermi liquid regime) can be obtained. Furthermore, the semianalytic nature of the solution permits a direct and fast calculation of the properties on a single workstation.

In addition, the general form of Eq. (6) can be written in the same way as Eq. (16) of Ref. [20], where the hybridization function $\Delta(\omega)$ depends on the full density of states of the conduction electrons $\rho(\omega)$ in the following form: $\Delta(\omega) = \pi V^2 \rho(\omega)$. Therefore, the approximation would be of interest for cases with nontrivial, frequency dependent, hybridization function, where the Bethe ansatz technique indeed cannot be applied.

Bethe ansatz equations of the impurity valence at zero magnetic field To compute the valence of the impurity at zero magnetic field and for arbitrary values of the parameters U, ϵ_d, Δ we start with the expressions (5.8) and (5.9) given by Wiegmann and Tsvelick in Refs. [2, 3].

$$\frac{U/2+\epsilon_d}{(2U\Delta)^{1/2}} = \frac{i}{\sqrt{2\pi}} \int_{-\infty}^{+\infty} \frac{d\omega}{\omega + i\eta} \frac{e^{-|\omega|/2 - i\omega Q}}{G^{(-)}(\omega)} \frac{1}{(-i\omega+\eta)^{1/2}} \tag{13}$$

$$n_d = 1 - \frac{i}{\sqrt{2\pi}} \int_{-\infty}^{+\infty} \frac{d\omega}{\omega + i\eta} \frac{e^{-|\omega|/2}}{G^{(-)}(\omega)} \times \int_{-\infty}^{+\infty} d\kappa\, e^{i\omega(g(\kappa)-Q)} \Delta(\kappa). \tag{14}$$

where the functions $G^{(-)}(\omega)$, $g(\kappa)$, and $\Delta(\kappa)$ are given by

$$G^{(-)}(\omega) = \sqrt{2\pi}\, \frac{(\frac{i\omega+\eta}{2\pi e})^{i\omega/2\pi}}{\Gamma(\frac{1}{2} + \frac{i\omega}{2\pi})},$$

$$g(\kappa) = \frac{(\kappa - \epsilon_d - U/2)^2}{2U\Delta},$$

$$\Delta(\kappa) = \frac{\Delta}{\pi} \frac{1}{(\kappa-\epsilon_d)^2 + \Delta^2},$$

with $\eta \to 0^+$. The equation in (13) fixes the value of Q that enters in the explicit calculation of the impurity occupation in (14).

The highly divergent nature of the integrand in Eq. (13) demands particular care in handling the limit $\eta \to 0^+$. In fact, using the identity $\frac{1}{\sqrt{-i\omega+\eta}} = \frac{1}{\sqrt{-i}} \frac{1}{\sqrt{\omega+i\eta}} \to \frac{1}{\sqrt{2|\omega|}}$ $(1 + i\, sgn(\omega))$ and taking explicitly the limit $\eta \to 0^+$ the RHS of (13), which we call $Z(Q)$, becomes

$$Z(Q) = \frac{i}{\sqrt{2\pi}} \int_{-\infty}^{+\infty} \frac{d\omega}{\omega+i\eta} \frac{e^{-|\omega|/2-i\omega Q}}{G^{(-)}(\omega)} \frac{1}{(-i\omega+\eta)^{1/2}} = \frac{i}{\sqrt{2\pi}} \int_{-\infty}^{+\infty} \frac{d\omega}{\sqrt{2|\omega|}} (1/\omega - i\pi\delta(\omega)) \times (1 + i\, sgn(\omega))\, H(\omega, Q)$$

with $H(\omega, Q) = \frac{e^{-|\omega|/2-i\omega Q}}{G^{(-)}(\omega)}|_{\eta\to 0^+} = \frac{e^{-i\omega Q}\,\Gamma(\frac{1}{2}+\frac{i\omega}{2\pi})}{\sqrt{2\pi}\,|\frac{\omega}{2\pi e}|^{i\omega/2\pi}\, e^{|\omega|/4}}$ and being the limit $H(0, Q) = 1/\sqrt{2}$, the argument has a nonintegrable singularity at $\omega = 0$. In order to avoid this singularity and make the integral tractable numerically, we subtract the singular part of $Z(Q)$ before taking the limit $\eta \to 0^+$.

Let us write the integral $Z(Q)$ in the following form

$$Z(Q) = \frac{i}{\sqrt{-2i\pi}} \int_{-\infty}^{+\infty} \frac{d\omega}{(\omega+i\eta)^{3/2}} \frac{e^{-|\omega|/2-i\omega Q}}{G^{(-)}(\omega)}. \tag{15}$$

Using the fact that

$$Z_s = \frac{ic}{\sqrt{-2i\pi}} \int_{-\infty}^{+\infty} \frac{d\omega}{(\omega + i\eta)^{3/2}} = 0 \tag{16}$$

we set $c = 1/G^{(-)}(0) = 1/\sqrt{2}$ and re-write $Z(Q) = Z(Q) - Z_s$ as follows

$$\begin{aligned} Z(Q) &= \frac{i}{\sqrt{-2i\pi}} \int_{-\infty}^{+\infty} \frac{d\omega}{(\omega + i\eta)^{3/2}} \left\{ H(\omega, Q) - \frac{1}{\sqrt{2}} \right\} \\ &= \frac{i}{2\sqrt{\pi}} \int_{-\infty}^{+\infty} d\omega \frac{1 + i\, sgn(\omega)}{\omega\sqrt{|\omega|}} \left\{ H(\omega, Q) - \frac{1}{\sqrt{2}} \right\}. \end{aligned} \tag{17}$$

In this way, the argument within the integral becomes regular.

We also map the infinite range of integration to a finite one by using

$$\begin{aligned} &\int_{-\infty}^{+\infty} d\omega\, f(\omega) \\ &= \int_0^{+\infty} d\omega \, \{f(\omega) + f(-\omega)\} \\ &= \int_0^1 dx \frac{1+x}{(1-x)^3} \left\{ f\left(\frac{x}{(1-x)^2}\right) + f\left(\frac{-x}{(1-x)^2}\right) \right\}. \end{aligned}$$

The change of variable was chosen so that the argument of the integral is smooth for $x \to 1$ ($\omega \to \infty$). By means of the above-mentioned transformations, the integral becomes suitable for numerical evaluation.

The integral in (14) is simpler and it can be evaluated in a more direct way. Calling $K(\omega) = \int_{-\infty}^{+\infty} d\kappa\, e^{i\omega(g(\kappa)-Q)} \Delta(\kappa)$, it becomes

$$\begin{aligned} n_d &= 1 - \frac{i}{\sqrt{2}\pi} \int_{-\infty}^{+\infty} \frac{d\omega}{\omega + i\eta} \frac{e^{-|\omega|/2}}{G^{(-)}(\omega)} K(\omega) \\ &= 1 - \frac{i}{\sqrt{2}\pi} \int_{-\infty}^{+\infty} d\omega \, (1/\omega - i\pi\delta(\omega)) \frac{e^{-|\omega|/2}}{G^{(-)}(\omega)} K(\omega) \\ &= 1 - \frac{i}{\sqrt{2}\pi} \left\{ \int_{-\infty}^{+\infty} d\omega \, \frac{e^{-|\omega|/2}}{\omega G^{(-)}(\omega)} K(\omega) - \frac{i\pi}{\sqrt{2}} \right\} \\ &= \frac{1}{2} + \frac{1}{\sqrt{2}\pi} \int_{-\infty}^{+\infty} d\omega \, \frac{e^{-|\omega|/2}}{\omega} \mathcal{I}m \left[\frac{K(\omega)}{G^{(-)}(\omega)} \right] \end{aligned} \tag{18}$$

Finally, we compute the principal part of the integral with the help of the following transformations

$$\begin{aligned} &\int_{-\infty}^{+\infty} d\omega\, f(\omega) \\ &= \int_0^{+\infty} d\omega \, \{f(\omega) + f(-\omega)\} \\ &= \int_0^1 dx \frac{1}{(1-x)^2} \left\{ f\left(\frac{x}{1-x}\right) + f\left(\frac{-x}{1-x}\right) \right\}. \end{aligned}$$

Acknowledgements This work was partially supported by PIP 00273, PIP 01060, and PIP 112-201101-00832 of CONICET, and PICT R1776 and PICT 2013-1045 of the ANPCyT, Argentina. We acknowledge financial support from the brazilian agencies CNPq and FAPERJ(CNE).

References

[1] P. W. Anderson, Phys. Rev. **124**, 41 (1961).
[2] P. B Wiegmann and A. M. Tsvelick, J. Phys. C **16**, 2281 (1983).
[3] A. M Tsvelick and P. B. Wiegmann, Adv. Phys. **32**, 453 (1983).
[4] K. G. Wilson, Rev. Mod. Phys. **47**, 773 (1975).
[5] R. Bulla, T. A. Costi, and T. Pruschke, Rev. Mod. Phys. **80**, 395 (2008).
[6] N. E. Bickers, Rev. Mod. Phys. **59**, 845 (1987).
P. Coleman, Phys. Rev. B **29**, 3035 (1983).
[7] T. S Kim and D. L. Cox, Phys. Rev. Lett. **75**, 1622 (1995); Phys. Rev. B **54**, 6494 (1996); Phys. Rev. B **55**, 12 594 (1997).
J. E. Han et al., Phys. Rev. Lett. **78**, 939 (1997)Q5.
V. L. Vildosola, M. Alouani, and A. M. Llois, Phys. Rev. B **71**, 184420 (2005).
P. Roura-Bas, V. Vildosola, and A. M. Llois, Phys. Rev. B **75**, 195129 (2007).
[8] N. Wingreen and Y. Meir, Phys. Rev. B **49**, 11040 (1994).
M. H. Hettler, J. Kroha, and S. Hershfield, Phys. Rev. Lett. **73**, 1967 (1994).
P. Roura-Bas, Phys. Rev. B **81**, 155327 (2010).
[9] S. Di Napoli, A. Weichselbaum, P. Roura-Bas, and A. A. Aligia, Phys. Rev. B **90**, 125149 (2014).
[10] P. Roura-Bas, L. Tosi, and A. A. Aligia, Phys. Rev. B **87**, 195136 (2013).
[11] L. Tosi, P. Roura-Â-Bas, and A. A. Aligia, Phys. Rev. B **88**, 235427 (2013).
[12] Th. Pruschke and N. Grewe, Z. Phys. B **74**, 439 (1989).
[13] K. Haule, S. Kirchner, J. Kroha, and P. Wölfle, Phys. Rev. B **64**, 155111 (2001).
[14] L. Tosi, P. Roura-Bas, A. M. Llois, and L. O. Manuel, Phys. Rev. B **83**, 073301 (2011).
[15] D. Jacob, K. Haule, and G. Kotliar, arXiv:0903.1274.
K. Haule, C.-H. Yee, and K. Kim, Phys. Rev. B **81**, 195107 (2010). S. Schmitt, Phys. Rev. B **82**, 155126 (2010).
[16] G. Kotliar, S. Y. Savrasov, K. Haule, V. S. Oudovenko, O. Parcollet, and C. A. Marianetti, Rev. Mod. Phys. **78**, 865 (2006).
[17] K. Kang and B. I. Min, Phys. Rev. B **54**, 1645 (1995).
[18] S. Inagaki, Prog. Theor. Phys. **62**, 1441 (1979).
[19] H. Keiter and J. C. Kimball, Int. J. Magn. **1**, 233 (1971).
[20] P. Roura-Bas, I. J. Hamad, and E. V. Anda, Phys. Status Solidi B **252**, 421 (2015).
[21] K. Edwards, A. C. Hewson, and V. Pandis, Phys. Rev. B **87**, 165128 (2013).
J.-D. Pillet, P. Joyez, Rok Žitko, and M. F. Goffman. Phys. Rev. B **88**, 045101 (2013).
J.-D. Pillet, C. H. L. Quay, P. Morfin, C. Bena, A. Levy Yeyati, and P. Joyez, Nat. Phys. **6**, 965 (2010).
[22] H. Kajueter and G. Kotliar, Phys. Rev. Lett. **77**, 131 (1996).
[23] A. A. Aligia, Phys. Rev. B **74**, 155125 (2006); and references therein.
[24] A. A. Aligia, J. Phys.: Condens. Matter **24**, 015306 (2012).
[25] A. A. Aligia, Phys. Rev. B **89**, 125405 (2014).

[26] A. C. Hewson, The Kondo Problem to Heavy Fermions (Cambridge University Press, Cambridge, 1993).
[27] F. D. M. Haldane, Phys. Rev. Lett. **40**, 416 (1978).
[28] In general, the position of the impurity level E_d is renormalized to E_d^*. In particular for large U, the position of the charge-transfer peak in the spectral density lies at E_d^* and is pushed upward with respect to E_d. Haldane calculated this shift using poor man's scaling with a high energy cutoff, which is the smallest between U and half the band width D [27].
[29] N. Andrei, K. Furuya, and J. H. Lowenstein, Rev. Mod. Phys. **55**, 331 (1983).

Q1 Please confirm that given names (red) and surnames/family names (green) have been identified correctly. Also provide the first name of all authors.
Q2 Please provide Fax number.
Q3 Please check changes made.
Q4 Please check changes made.
Q5 Please provide the list of all authors if available.

[30] M. Höck and J. Schnack, Phys. Rev. B **87**, 184408 (2013).
[31] A. A. Aligia, C. A. Balseiro, and C. R. Proetto, Phys. Rev. B **33**, 6476 (1986).
[32] S. Amasha, A. J. Keller, I. G. Rau, A. Carmi, J. A. Katine, H. Shtrikman, Y. Oreg, and D. Goldhaber-Gordon, Phys. Rev. Lett. **110**,046604 (2013).
L. Tosi, P. Roura-Bas, and A. A. Aligia, J. Phys.: Condens. Matter **27**, 335601 (2015), and references therein.
[33] S. Kubatkin, A. Danilov, M. Hjort, J. Cornil, J. L, Brédas, N. Stuhr-Hansen, P. Hedegård, and Th. Bjørnholm, Nature **425**, 699 (2003).

USING e-ANNOTATION TOOLS FOR ELECTRONIC PROOF CORRECTION

WILEY

Required software to e-Annotate PDFs: Adobe Acrobat Professional or Adobe Reader (version 8.0 or above). (Note that this document uses screenshots from Adobe Reader X)
The latest version of Acrobat Reader can be downloaded for free at: http://get.adobe.com/reader/

Once you have Acrobat Reader open on your computer, click on the Comment tab at the right of the toolbar:

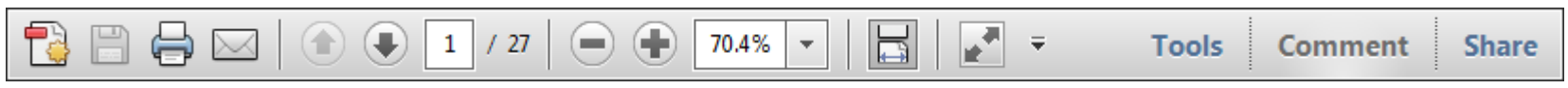

This will open up a panel down the right side of the document. The majority of tools you will use for annotating your proof will be in the Annotations section, pictured opposite. We've picked out some of these tools below:

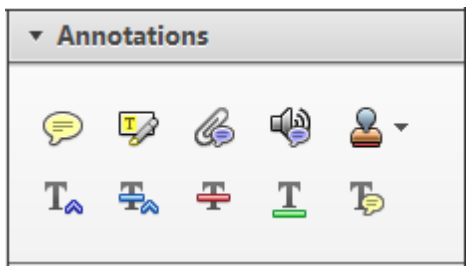

1. Replace (Ins) Tool – for replacing text.

Strikes a line through text and opens up a text box where replacement text can be entered.

How to use it

- Highlight a word or sentence.
- Click on the Replace (Ins) icon in the Annotations section.
- Type the replacement text into the blue box that appears.

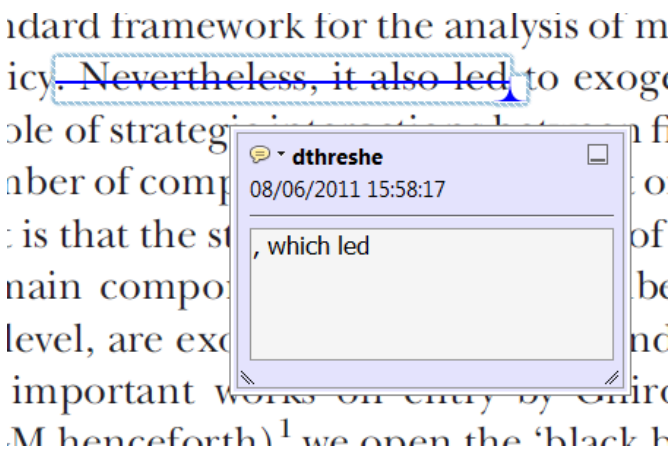

2. Strikethrough (Del) Tool – for deleting text.

Strikes a red line through text that is to be deleted.

How to use it

- Highlight a word or sentence.
- Click on the Strikethrough (Del) icon in the Annotations section.

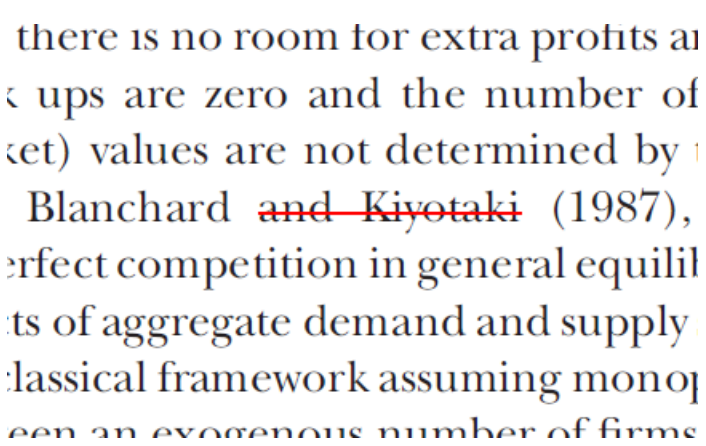

3. Add note to text Tool – for highlighting a section to be changed to bold or italic.

Highlights text in yellow and opens up a text box where comments can be entered.

How to use it

- Highlight the relevant section of text.
- Click on the Add note to text icon in the Annotations section.
- Type instruction on what should be changed regarding the text into the yellow box that appears.

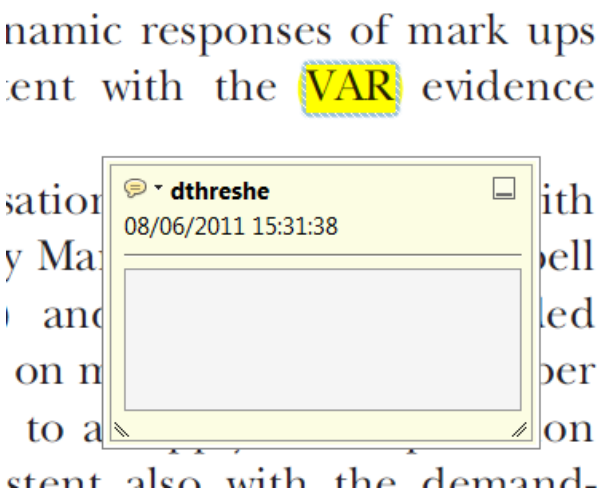

4. Add sticky note Tool – for making notes at specific points in the text.

Marks a point in the proof where a comment needs to be highlighted.

How to use it

- Click on the Add sticky note icon in the Annotations section.
- Click at the point in the proof where the comment should be inserted.
- Type the comment into the yellow box that appears.

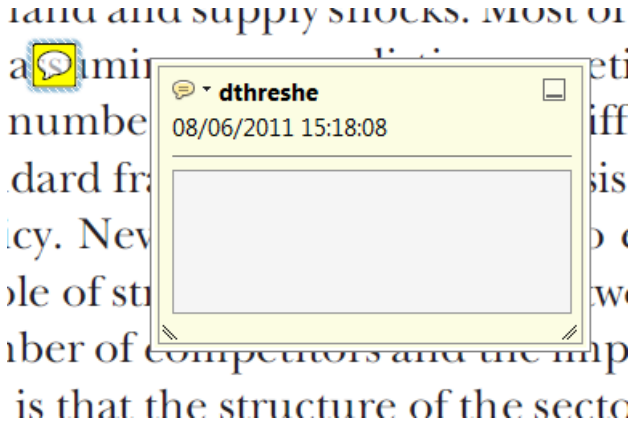

USING e-ANNOTATION TOOLS FOR ELECTRONIC PROOF CORRECTION

5. Attach File Tool – for inserting large amounts of text or replacement figures.

Inserts an icon linking to the attached file in the appropriate pace in the text.

How to use it

- Click on the Attach File icon in the Annotations section.
- Click on the proof to where you'd like the attached file to be linked.
- Select the file to be attached from your computer or network.
- Select the colour and type of icon that will appear in the proof. Click OK.

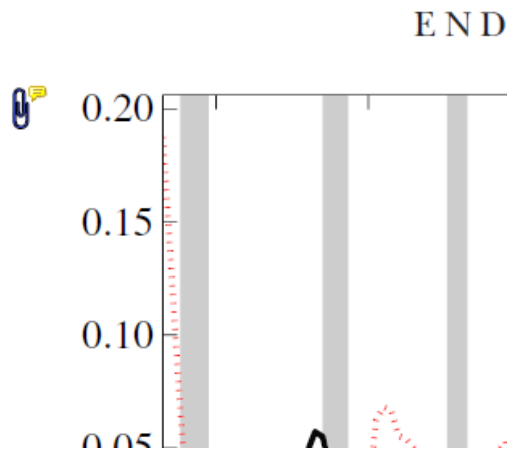

6. Add stamp Tool – for approving a proof if no corrections are required.

Inserts a selected stamp onto an appropriate place in the proof.

How to use it

- Click on the Add stamp icon in the Annotations section.
- Select the stamp you want to use. (The Approved stamp is usually available directly in the menu that appears).
- Click on the proof where you'd like the stamp to appear. (Where a proof is to be approved as it is, this would normally be on the first page).

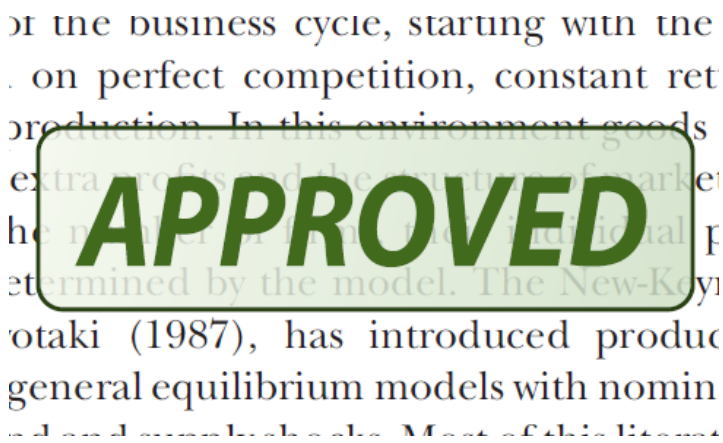

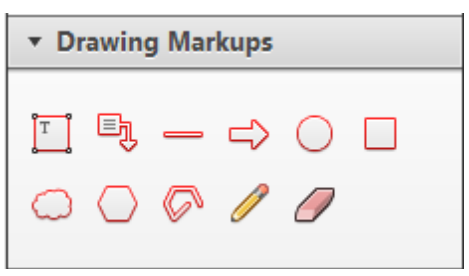

7. Drawing Markups Tools – for drawing shapes, lines and freeform annotations on proofs and commenting on these marks.

Allows shapes, lines and freeform annotations to be drawn on proofs and for comment to be made on these marks..

How to use it

- Click on one of the shapes in the Drawing Markups section.
- Click on the proof at the relevant point and draw the selected shape with the cursor.
- To add a comment to the drawn shape, move the cursor over the shape until an arrowhead appears.
- Double click on the shape and type any text in the red box that appears.

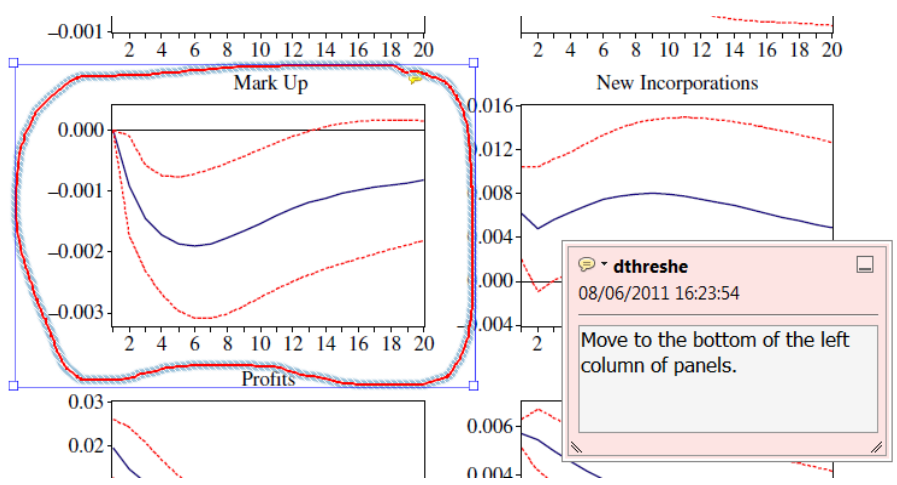

For further information on how to annotate proofs, click on the Help menu to reveal a list of further options:

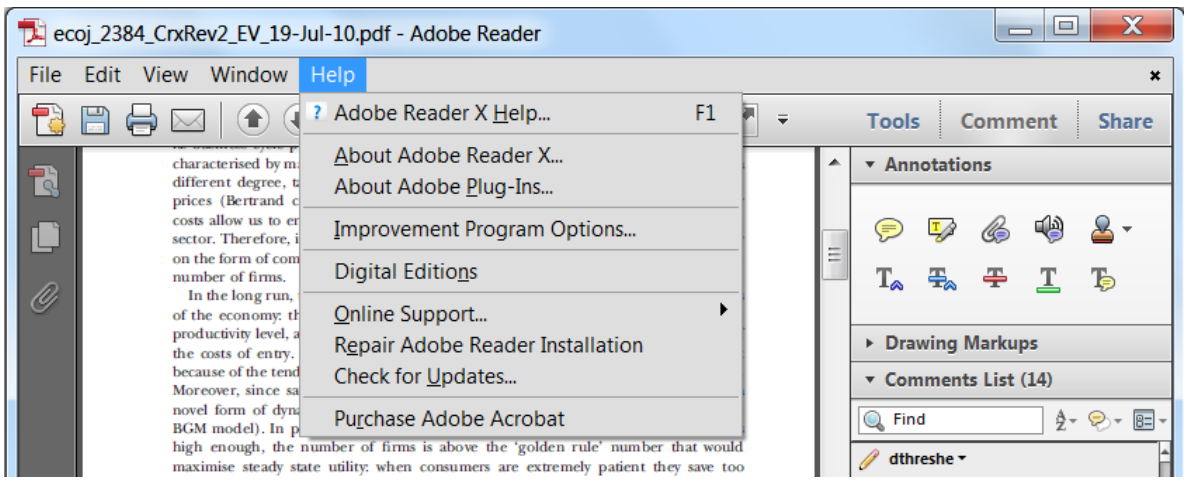

physica status solidi b
www.pss-b.com
basic solid state physics

Order Form

2015

WILEY-VCH GmbH & Co. KGaA
physica status solidi
Rotherstrasse 21
10245 Berlin
Germany
TEL +49 (0) 30–47 03 13 31
FAX +49 (0) 30–47 03 13 34
E-MAIL pssb.proofs@wiley-vch.de

WILEY-VCH

Please complete this form and return it by e-mail or FAX.

Article No.

Author/Title

e-mail address

Required Fields may be filled in using Adobe Reader

Color Print Authorization

Please bill me for

☐ color print figures (total number of color figures)

❒ YES, please print Figs. No. ☐ in color.

❒ NO, please print all color figures in black/white.

Reprints/Issues/PDF Files/Posters

Whole issues, reprints and PDF files (300 dpi) for an unlimited number of printouts are available at the rates given on the next page. Reprints and PDF files can be ordered before *and after* publication of an article. All reprints will be delivered in full color, regardless of black/white printing in the journal.

Reprints

Please send me and bill me for

☐ full color reprints with color cover

☐ full color reprints with personalized color cover

Issues

Please send me and bill me for

☐ entire issues

Customized PDF-Reprint

Please send me and bill me for

❒ a PDF file (300 dpi) for an unlimited number of printouts **with customized color cover sheet.**

The PDF file will be sent to your e-mail address.

Send PDF file to:

Please note that posting of the final published version on the open internet is not permitted. For author rights and re-use options, see the Copyright Transfer Agreement at http://www.wiley-vch.de/cta/ps-global.

Cover Posters

Posters are available of all the published covers in two sizes (see attached price list). **Please send me and bill me for**

☐ A2 (42 × 60 cm/17 × 24in) posters

☐ A1 (60 × 84 cm/24 × 33in) posters

Mail reprints and/or issues and/or posters to (no P.O. Boxes):

VAT number:

Information regarding VAT

Please note that from German sales tax point of view, the charge for **Reprints, Issues or Posters** is considered as **"supply of goods"** and therefore, in general, such delivery is subject to German VAT. However, this regulation has no impact on customers located outside of the European Union. Deliveries to customers outside the Community are automatically tax-exempt. Deliveries within the Community to institutional customers outside of Germany are exempted from German tax (VAT) only if the customer provides the supplier with his/her VAT number.

The VAT number (value added tax identification number) is a tax registration number used in the countries of the European Union to identify corporate entities doing business there. It starts with a country code (e.g. FR for France, GB for Great Britain) and follows by numbers.

The charges for publication **of front/back/inside cover pictures, color figures or frontispieces** are considered to be **"supply of services"** and therefore subject to German VAT. However, if you are an institutional customer outside Germany, the tax can be waived if you provide us with the VAT number of your company. Non-EU customers may have a VAT number starting with "EU" instead of their country code if they are registered with the EU tax authorities. If you do not have an EU VAT number and you are a taxable person doing business in a non-EU country, please provide certification from your local tax authorities confirming that you are a taxable person under local tax law. Please note that the certification must confirm that you are a taxable person and are conducting an economic activity in your country. **Note:** Certifications confirming that you are a tax-exempt legal body (non-profit organization, public body, school, political party, etc.) in your country do not exempt you from paying German VAT.

Purchase Order No.:

Terms of payment:

❒ Please send an invoice ❒ Cheque is enclosed

❒ **VISA, MasterCard and AMERICAN EXPRESS.**

Please use this link (Credit Card Token Generator) to create a secure Credit Card Token and include this number in the form instead of the credit card data.

https://www.wiley-vch.de/editorial_production/index.php

CREDIT CARD TOKEN NUMBER:

Send invoice to:

Signature _____

Date _____

Please use this form to confirm that you are prepared to pay your contribution.

Please sign and return this page.

You will receive an invoice following the publication of your article in the journal issue.

Price List – pss (b) 2015

Reprints/Issues/PDF-Files/Posters

WILEY-VCH

The prices listed below are valid only for orders received in the course of 2015. Minimum order for reprints is 50 copies. **Reprints can be ordered before *and after* publication of an article. All reprints are delivered with color cover and color figures**. If more than 500 copies are ordered, special prices are available upon request.

Single issues are available to authors at a reduced price.

The prices include mailing and handling charges. All prices are subject to local VAT/sales tax.

Reprints with color cover	Price for orders of (in Euro)					
Size (pages)	50 copies	100 copies	150 copies	200 copies	300 copies	500 copies*
1– 4	345	395	425	445	548	752
5– 8	490	573	608	636	784	1077
9–12	640	739	786	824	1016	1396
13–16	780	900	958	1004	1237	1701
17–20	930	1070	1138	1196	1489	2022
for every additional 4 pages	147	169	175	188	231	315
for personalized color cover	**190**	**340**	**440**	**650**	**840**	**990**

PDF file (300 dpi, unlimited number of printouts, customized cover sheet)	€ 330
Issues	€ 36 per copy for up to 10 copies.*
Cover Posters	• A2 (42 × 60 cm/17 × 24in) € 49 • A1 (60 × 84 cm/24 × 33in) € 69

*Prices for more copies available on request.

Special offer: If you order 100 or more reprints you will receive a pdf file (300 dpi, unlimited number of printouts, color figures) and an issue for free.

Color figures

If your paper contains **color figures**, please notice that, generally, these figures will appear in color in the online PDF version and all reprints of your article at no cost. The print version of the figures in the journal hardcopy will be black/white unless the author explicitely requests a color print publication and contributes to the additional printing costs.

	Approximate color print figure charges
First figure	€ 495
Each additional figure	€ 395 Special prices for more color print figures on request

If you wish color figures in print, please answer the **color print authorization** questions on the order form.